

Communication

Reaction of Triazolic Aldehydes with Diisopropyl Zinc: Chirality Dissipation versus Amplification

Oleg A. Mikhaylov¹, Elena Sh. Saigitbatalova², Liliya Z. Latypova², Almira R. Kurbangaliev^{2,*} 
and Ilya D. Gridnev^{1,*} ¹ N. D. Zelinsky Institute of Organic Chemistry, Leninsky Prosp. 47, 119991 Moscow, Russia² Biofunctional Chemistry Laboratory, A. Butlerov Institute of Chemistry, Kazan Federal University, 18 Kremlyovskaya Street, 420008 Kazan, Russia

* Correspondence: akurbang@kpfu.ru (A.R.K.); ilyaiochem@gmail.com (I.D.G.)

Abstract: The phenomenon of amplifying asymmetric autocatalysis (AAA) has recently been restricted to alkylation of several specific substrates with diisopropyl zinc (Soai reaction). Targeting the extension of the scope of this phenomenon, we studied the reaction of triazolic aldehydes with diisopropyl zinc. Experiments demonstrated a diversity of results for the dissipation of chirality, conserving the existent ee and spontaneous chirality generation. Computational analysis showed that depending on the level of oligomerization of the catalyst, one could expect amplification (monomeric catalyst) while maintaining the existing chirality (dimeric catalyst) or dissipation of chirality (tetrameric catalyst). These findings are promising for the elaboration of synthetic protocols controlling chirality generation. In addition, three optically active triazolic alcohols were characterized.

Keywords: Soai reaction; chirality amplification; diisopropyl zinc; DFT computations; triazoles



Citation: Mikhaylov, O.A.; Saigitbatalova, E.S.; Latypova, L.Z.; Kurbangaliev, A.R.; Gridnev, I.D. Reaction of Triazolic Aldehydes with Diisopropyl Zinc: Chirality Dissipation versus Amplification. *Symmetry* **2023**, *15*, 1382. <https://doi.org/10.3390/sym15071382>

Academic Editors: Qiang Sha and Ying He

Received: 15 June 2023

Revised: 3 July 2023

Accepted: 5 July 2023

Published: 7 July 2023



Copyright: © 2023 by the authors. Licensee MDPI, Basel, Switzerland. This article is an open access article distributed under the terms and conditions of the Creative Commons Attribution (CC BY) license (<https://creativecommons.org/licenses/by/4.0/>).

1. Introduction

The discovery of the autocatalytic and autoamplifying Soai reaction [1] made a strong impression on the chemists of that time. The capability of a chiral catalyst to reproduce and amplify its chirality inevitably results in an aptitude of this system for spontaneous chirality generation [2], which is extremely interesting from several points of view. First, this phenomenon is closely connected with the fundamental problem of the emergence of chiral life on Earth [3]. Not any less important are the conceivable synthetic applications if the regularities of this process could be elucidated to a sufficient extent. Additionally, the analysis of the structural requirements necessary for the reagents to promote such a complicated event opens new perspectives for understanding the details of molecular behavior in sophisticated and challenging systems [4].

The inherently stochastic character of spontaneous chirality generation implies an exponential increase in the number of experiments required to reach a reliable conclusion on the authentic event. However, the principal question of the authenticity of this phenomenon in a system demonstrating asymmetric autoamplification was solved positively 20 years ago in a series of publications [5–7]. On the other hand, Soai's group provided ample evidence for the aptitude of various chiral additives to initiate the induction of chirality with the handedness determined by the structure of the inductor [8]. It is evident that both these events require the same thing, i.e., the presence of AAA (Amplifying Asymmetric Autocatalysis) [4].

These considerations lead to an important conclusion: if some reactions without chiral additives provide a scalemic product, we do not need to determine whether true absolute asymmetric synthesis was observed in this particular experiment or if this event was caused by the presence of tiny amounts of a chiral inductor of unspecified origin. In any case, AAA is effective, and if it would be absolutely necessary, real spontaneous chirality generation can be confirmed for this system.

Another important feature of the Soai reaction is its strict requirements regarding the structure of reagents. Thus, so far, only diisopropyl zinc has been successfully applied as an alkylating reagent. Structures of the effective substrates are also rigorously limited by combination of a pyrimidinic core, acetylenic linker and bulky terminal anchor (*t*-Bu, Me₃Si, adamantyl). These limitations arise from a sophisticated tetrameric structure of the amplifying autocatalyst [9]; any simplification of the structure leads to a considerable worsening of the performance with the notable exception of a recently reported pyridine-based molecule with the same linker and anchor [10].

Numerous possibilities of AAA are conceivable for oligomeric catalysts following the Frank–Decker scheme for autoamplification or due to the reservoir effect for the monomeric catalyst [11]. As we were interested in extending the structural scope of autocatalytic and autoamplifying reactions, we have launched a project to search for new examples of such transformations.

2. Materials and Methods

2.1. Experimental Details

Diisopropylzinc 1M solution in toluene (Sigma-Aldrich, Schnelldorf, Germany) was used as received without further purification. All solvents were purified and distilled using standard procedures. Analytical thin-layer chromatography (TLC) was carried out on Sorbfil PTLC-AF-A-UF plates using acetone–chloroform (1:4) as the eluent and UV light (254 nm) as the visualizing agent. Silica gel 60A (Acros Organics, 400–230 mesh, 0.040–0.063 mm) was used for open-column chromatography. Melting points were recorded with a Boëtius melting point instrument and are uncorrected. NMR spectra were measured on a Bruker Avance 300 spectrometer at 300.13 MHz (¹H) and 75.47 MHz (¹³C), Bruker Avance 600 spectrometer at 600.13 MHz (¹H) and 150.90 MHz (¹³C) at 20 °C in the deuterated chloroform. The chemical shifts (δ) are expressed in parts per million (ppm) and are calibrated using residual undeuterated solvent peak as an internal reference (CDCl₃: δ_{H} 7.26, δ_{C} 77.16). All coupling constants (*J*) are reported in Hertz (Hz), and multiplicities are indicated as follows: s (singlet), d (doublet) and m (multiplet). High-resolution mass spectra (HRMS) were obtained through electrospray ionization (ESI) with positive (+) ion detection on a Bruker micrOTOF–QIII quadrupole time-of-flight mass spectrometer. The ee measurements were performed via HPLC analysis. HPLC analysis was performed on an HPLC system equipped with chiral stationary phase columns (AD-H, AS-H, OD-H, OJ-H), detection at 220 or 254 nm. Synthetic procedures and characterization details for the new compounds can be found in the Supplementary Materials.

2.2. Chemical Synthesis

1-Benzyl-1*H*-1,2,3-triazole-4-carbaldehyde (**1**) [12], 1-phenyl-1*H*-1,2,3-triazole-4-carboxaldehyde (**2**) and 1-(4-chlorophenyl)-1*H*-1,2,3-triazole-4-carboxaldehyde (**3**) [13] were synthesized according to the known methods.

All reactions were carried out using standard Schlenk techniques under argon atmosphere.

2.3. Computational Details

Geometry optimizations were performed without any symmetry constraints (C1 symmetry) using the ω B97XD functional [14] as implemented in the Gaussian09 software package [15]. Frequency calculations were undertaken to confirm the nature of the stationary points, yielding one imaginary frequency for all transition states (TSs) and zero for all minima. Constrained energy hypersurface scans were conducted to investigate the molecular reactivity and to locate viable reaction channels. Where low-lying barriers were estimated, frequency calculations were performed at the crude saddle points, and the obtained force constants were used to optimize the transition-state structures employing the Berny algorithm [16]. All atoms were described with a 6-31G** basis set in the geometry optimization and frequency calculation [17–22]. Non-specific solvation was introduced by using the SMD continuum model [23] (acetonitrile).

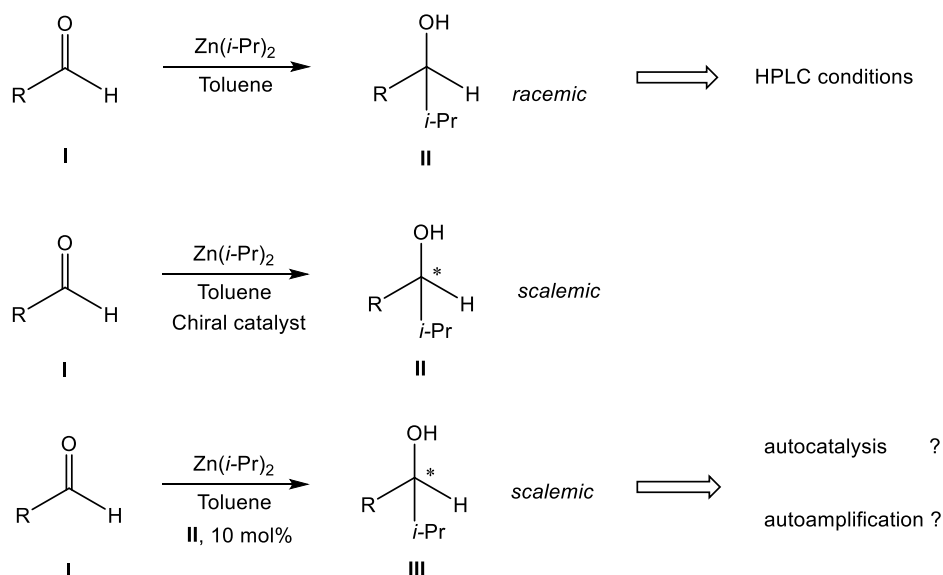
3. Results

3.1. Development of a Strategy for the Screening of Promising Substrates

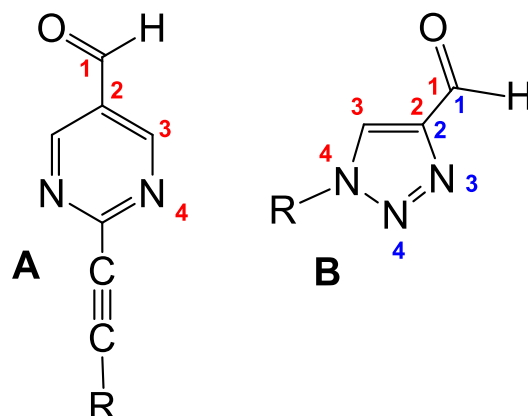
Despite the extensive development of various enantioselective reactions seen at the present time, practically all of them require more or less arbitrary optimization of the reaction conditions, i.e., structure of the catalyst, solvent, reaction temperature, pressure, additives, etc. Among a dozen chiral catalysts, most providing a high performance in some already-known transformations; only one or two are actually working in a newly discovered asymmetric catalytic reaction. Before these winners are actually found, the tables listing yields and ee values may look rather empty, and only persistence in this random search may result in a happy finding.

In our case, it is impossible to incorporate the same approach to each of the substrate candidates for AAA, since it would require too much time. Nevertheless, we need more readily available results that would justify the transfer of a reaction into step two of the screening. We decided to check if the ability to effectuate an autocatalytic reaction can serve as such a criterion without making the whole screening process unreasonably tiresome.

To do this, we designed and synthesized, to an extent, a small series of compounds similar to the effective substrates of the Soai reaction and used them in the following trial sequence (Schemes 1 and 2).



Scheme 1. Trial sequence for searching for perspective compounds for autoamplification (asterisk means asymmetric carbon atom).

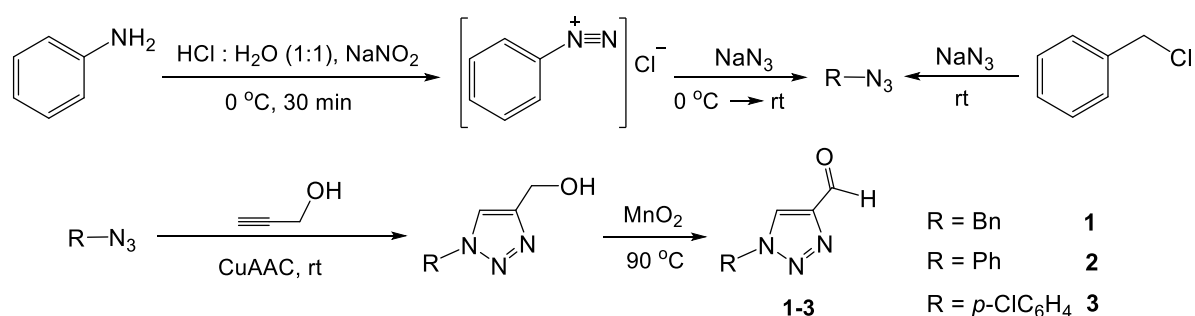


Scheme 2. Comparison of the general formula of Soai aldehydes (A) and perspective 1,2,3-triazoles (B).

3.2. Design and Synthesis of the Perspective Substrates

In looking for possible perspective substrates, we were attracted by the 1,2,3-triazole skeleton since it presents the possibility of introducing the aldehyde group into 1,4-position with the aromatic nitrogen atom (Scheme 2). Additionally, substituted triazoles find numerous applications in pharmaceuticals, supramolecular chemistry, organic synthesis, chemical biology and industry [24–29]. Moreover, compounds containing the 1,2,3-triazole moiety show a wide spectrum of biological activity [30] including antitubercular [31], antibacterial [32], antimalarial [33], anti-HIV [34], anticancer [35], antiallergic [36] and antifungal [37] properties.

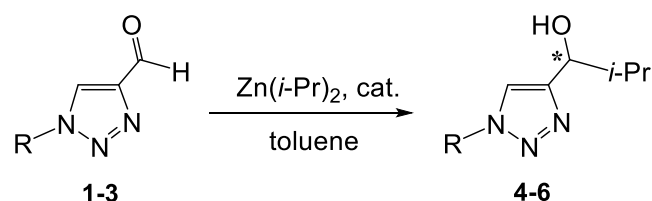
A series of aldehydes with triazole fragments were prepared using the recently described procedures [12,13] (Scheme 3).



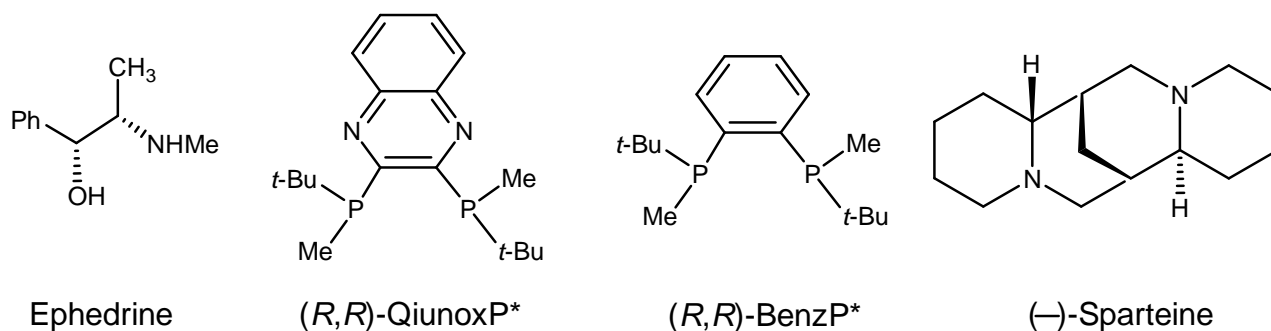
Scheme 3. Synthesis of substituted 1,2,3-triazole aldehydes 1–3.

3.3. Reactions of Compounds 1–3 with Diisopropylzinc

Compounds 1–3 react with excess diisopropylzinc in the presence of a chiral catalyst or without any catalyst (Schemes 4 and 5, Table 1).



Scheme 4. Catalytic reactions of compounds 1–3 with diisopropyl zinc (asterix means asymmetric carbon atom).



Scheme 5. Structural formula of the chiral catalysts (asterix means asymmetric carbon atom).

Table 1. Reactions of compounds 1–3 with diisopropyl zinc.

Entry	Compound Number	Cat	Ratio Ald:Zn(<i>i</i> -Pr) ₂ :Cat	Conditions	Yield, %	ee, %
1	R = Bn (1)	none	1:10	r.t., 4 h	43	3
2			1:10	reflux 0.1 h (NMR tube)	25	41
3		Ephedrine	1:10:0.2	80 °C, 6 h	20	35
4			1:10:0.1	80 °C, 4 h	33	37
5			1:10:0.1	reflux, 0.1 h (NMR tube)	29	10
6		(<i>R,R</i>)-QiunoxP *	1:10:0.1	80 °C, 4 h	25	2
7		(<i>R,R</i>)-BenzP *	1:10:0.1	80 °C, 4 h	30	20
8		1, 20% ee	1:10:0.2	r.t., overnight	11	0
9		1, 37% ee	1:10:0.2	80 °C, 4 h	30	25
10	R = Ph (2)	none	1:10	r.t., 4 h	48	0
11		Ephedrine	1:10:0.1	r.t., 1 h	40	27
12		(<i>R,R</i>)-QiunoxP *	1:10:0.1	r.t., 1 h	75	2
13		(<i>R,R</i>)-BenzP *	1:10:0.1	r.t., overnight	24	13
14		(-)-Sparteine	1:10:0.1	r.t., 4 h	13	3
15		2, 13% ee	1:10:0.2	r.t., 3 h	48	0
16		2, 27% ee	1:10:0.2	r.t., overnight	47	0
17	R = <i>p</i> -ClC ₆ H ₄ (3)	none	1:10	r.t., 4 h	37	10
18			1:10	r.t., overnight	52	11
19			1:10	reflux, 0.1 h (NMR tube)	21	0
20		Ephedrine	1:20:0.1	r.t., overnight	31	33
21		(<i>R,R</i>)-QiunoxP *	1:10:0.1	reflux, 0.1 h (NMR tube)	25	15
22		(<i>R,R</i>)-BenzP *	1:10:0.1	reflux, 0.1 h (NMR tube)	20	9
23		3, 33% ee	1:10:0.2	r.t., overnight	53	5

Asterix means asymmetric carbon atom.

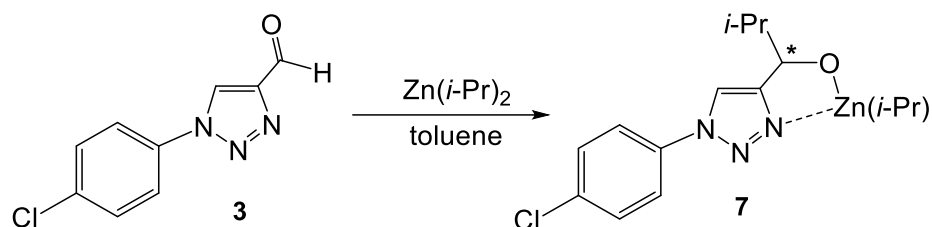
Analysis of the experimental data collected in Table 1 leads to the following conclusions:

- A significant accelerating effect of a catalyst was observed only in the reaction of **2** catalyzed by (*R,R*)-QuinoxP* (entry 12). For **1** and **3**, the highest yields were obtained in the non-catalyzed reactions (entries 1, 18).
- Among the applied chiral catalysts, only ephedrine led to the formation of notably optically enriched products (entries 3–5, 11, 20). Even in these cases, a negative non-linear effect was observed, since the ee of the products was significantly lower than the ee of the catalyst.
- Autocatalysis was not observed: compare entries 1 and 8; 10 and 15, 16; 17, 18 and 23.
- Some of the results of the autocatalytic reactions roughly correspond to preserving the ee of the catalyst diluted by a larger amount of the non-chiral product (entries 9, 23). Other results indicate dissipation of chirality (entries 8, 15, 16).
- Spontaneous chirality generation was observed for substrates **1** and **3** (entries 1, 2, 17, 18).

We assumed that these findings might be a result of different mechanisms operating under dissimilar reaction conditions. We leave the accurate elucidation of these conditions, extending the scope of the substrates, experimental studies of the reaction pools and kinetic simulations for a full paper. In this preliminary communication, we would like to perform a demonstration of principle by locating computationally probable catalysts in the reaction pool that are capable of exhibiting either positive or negative non-linear effects in one of the reactions under study. The former species might be operative in the synthetic protocol, resulting in the spontaneous generation of chirality, whereas the latter one might be responsible for the dissipation of the enantiomeric excess in the reactions with the pre-formed catalyst.

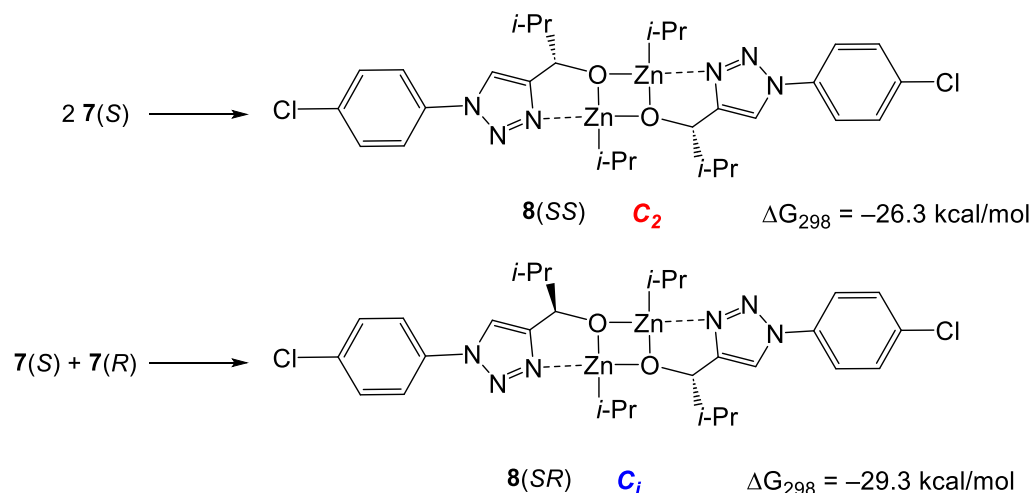
3.4. Computational Analysis of the Reaction of Aldehyde 3 with Diisopropyl Zinc

A primary product of the alkylation of aldehyde 3 is alcoholate 7 (Scheme 6). From previous studies, it is known that similar alcoholates readily form oligomers that play an important role in the autocatalysis. We have computed possible oligomerization pathways for 7.



Scheme 6. Formation of monomeric alcoholate 7 (asterix means asymmetric carbon atom).

Similarly to the previously studied cases [9,38], the dimerization of 7 is strongly exergonic and leads to the formation of the square dimers 8(SS) and 8(RS). However, unlike the previous cases, in which the stabilities of the homo- and heterochiral dimers were practically equal, 8(RS) was computed to be more stable than 8(SS) for 3.0 kcal/mol (Scheme 7).



Scheme 7. Formation of square dimers 8(SS) and 8(SR).

The greater stability of 8(RS) is due to a larger number of CH \cdots HC interactions across the Zn₂O₂ square (Figure 1) arising due to conformational restrictions created by the coordination binding of Zn with the nitrogen atoms in position 2 of the triazolic rings.

Importantly, the significantly higher stability of the heterochiral dimer 8(SR) implies a possibility of a positive NLE via the so-called “reservoir effect”. This means that the catalyst is a monomer capable of catalyzing an enantioselective reaction, and the minor enantiomer is deactivated via its accumulation in the more stable dimer [11]. We investigated this possibility computationally (Scheme 8).

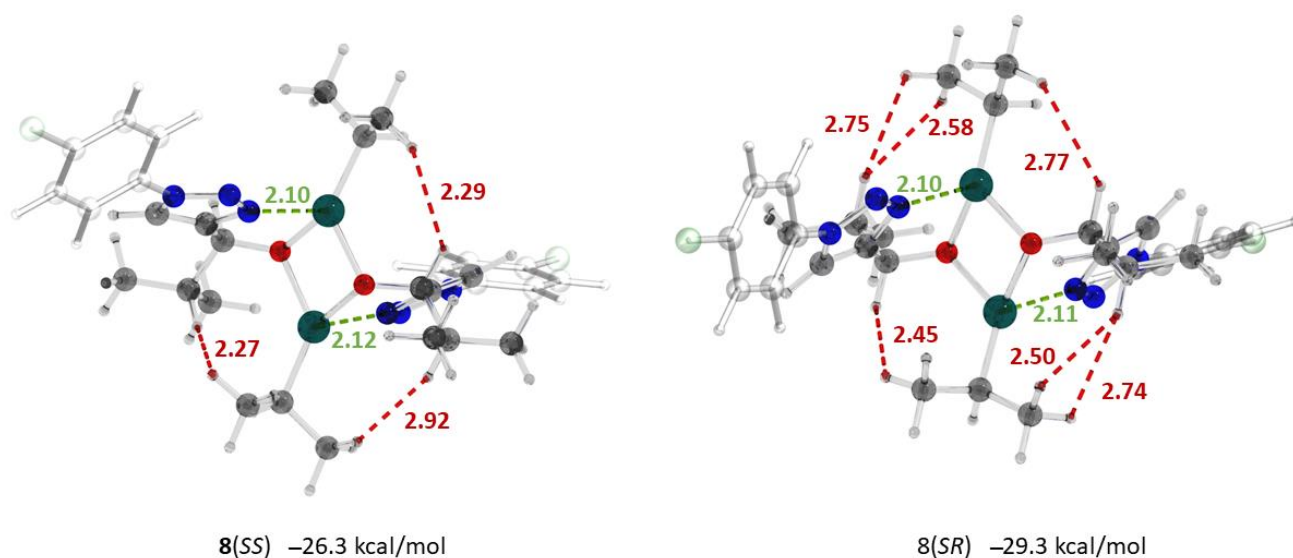


Figure 1. Optimized structures, important interatomic distances (Å) and relative Gibbs free energies (ΔG_{298} , relative to 2 **7(S)**) of the square dimers **8(SS)** and **8(SR)**. Atoms: gray—carbon; light gray—hydrogen; red—oxygen; blue—nitrogen; green—chlorine; turquoise—zinc. Interatomic distances: red—CH \cdots HC; green—Zn—N.

Diisopropyl zinc coordinates in a chelate way to the oxygen and N(2) atoms of **7(S)**, yielding adduct **9(S)**. Aldehyde **3** coordinates to the Zn atom, yielding **10**. The isopropyl groups in **10** can attack the prochiral plane from the opposite sides via **TS1(S)** or **TS1(R)**, yielding the adducts **7(S) • 7(S)** or **7(S) • 7(R)**, respectively. Since **TS1(R)** is 7.2 kcal/mol less stable than **TS1(S)** due to the significantly smaller number of stabilizing weak interactions between the substrate and the catalyst compared to **TS1(S)** (Figure 2), amplification of chirality takes place via predominant formation of **7(S) • 7(S)**.

Thus, we concluded that AAA is possible for compound **7** via the “reservoir” mechanism through the combination of the greater stability of the heterochiral dimer **8(SR)** compared to **8(SS)** and the enantioselective alkylation catalyzed by the monomeric alcoholate.

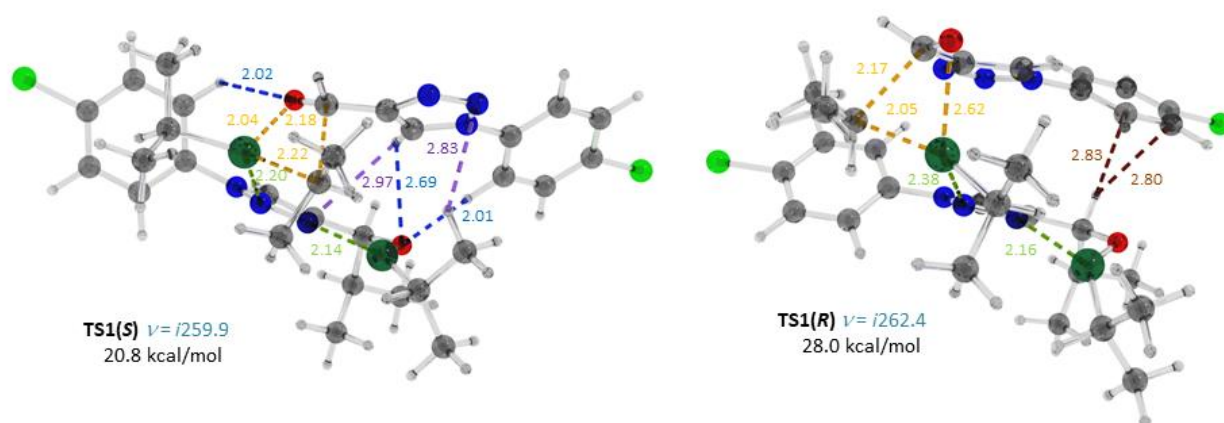
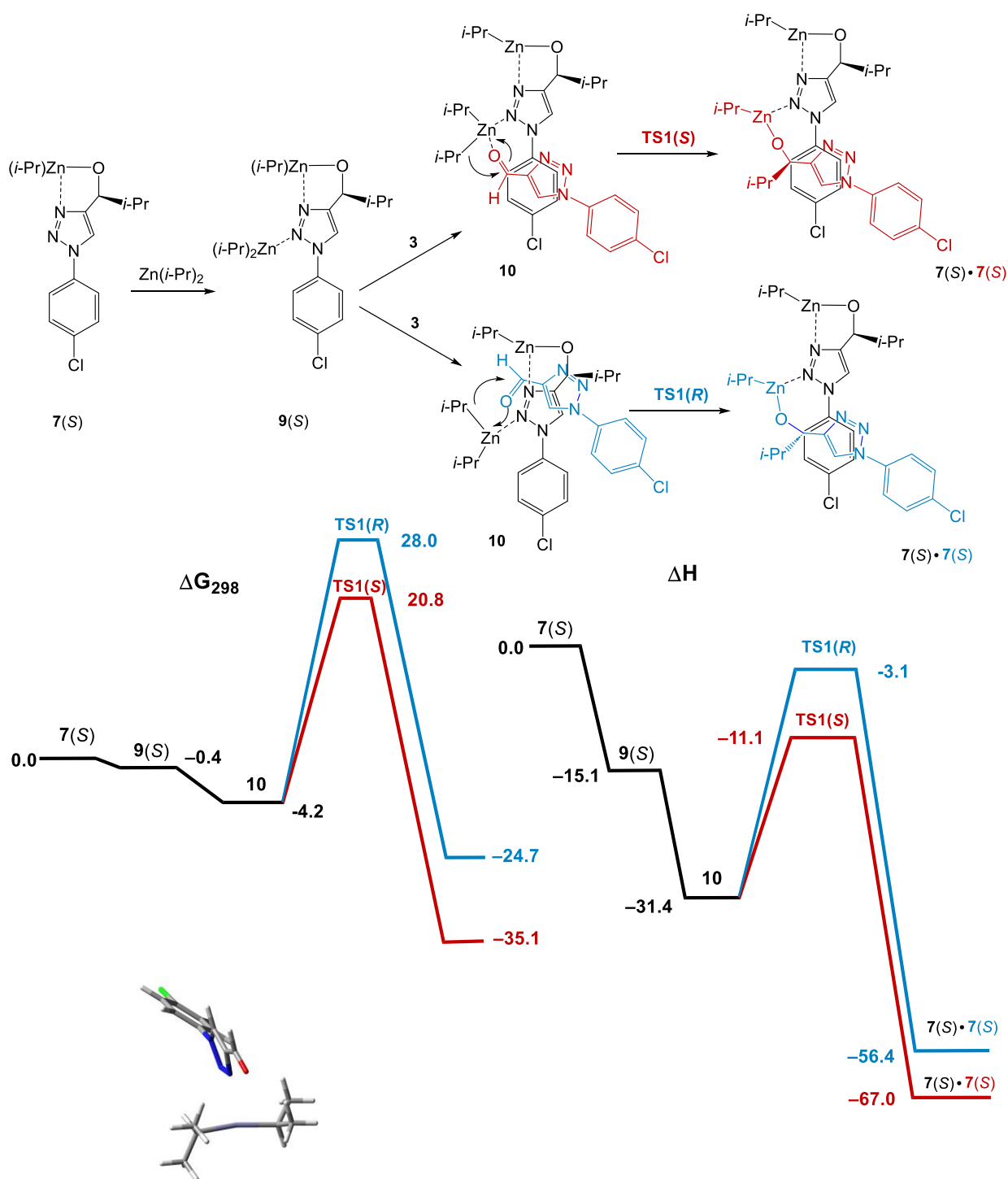


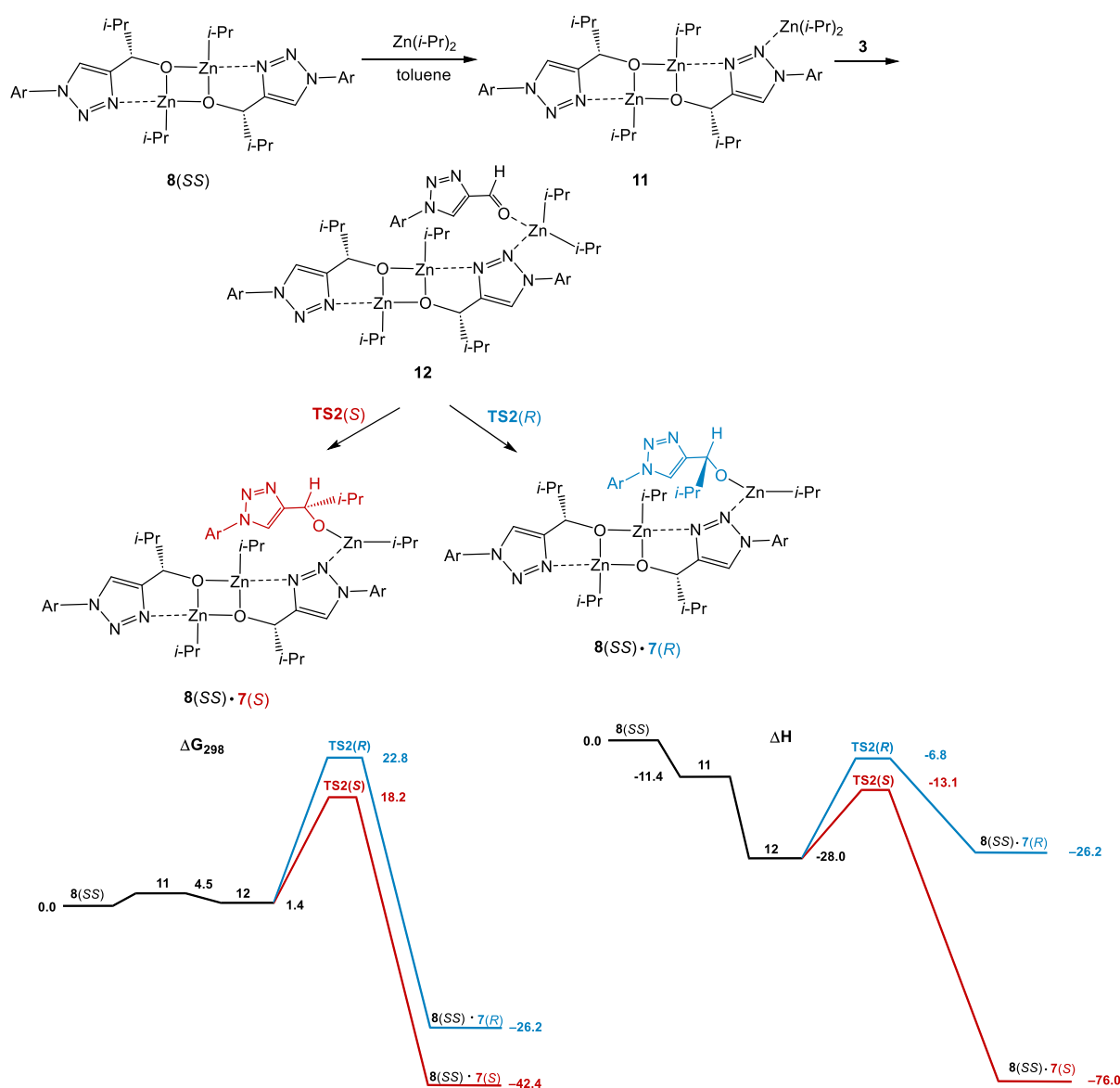
Figure 2. Optimized structures, important interatomic distances (Å) and Gibbs free energies (ΔG_{298} , relative to **7(S)** + Zn(*i*-Pr) $_2$ + **3**) of the transition states **TS1(S)** and **TS1(R)**. Atoms: gray—carbon; light gray—hydrogen; red—oxygen; blue—nitrogen; green—chlorine; turquoise—zinc. Interatomic distances: yellow—forming bonds and those being broken; green—Zn—N; blue: CH \cdots O; violet, CH \cdots N; brown CH \cdots π .



Coordination mode of aldehyde in 10

Scheme 8. Computational results (ΔG_{298} and ΔH relative to 7(S) + Zn(*i*-Pr)₂ + 3) for the reaction of diisopropyl zinc with aldehyde 3 catalyzed by 7(S). AAA via reservoir mechanism.

It is evident that very similar transition states can be found for the reactions catalyzed by the resting-state species, i.e., square dimers 8 (e.g., Scheme 9, Figure 3). In that case, the reservoir effect is absent and the enantiomeric pairs, 8(SS) and 8(RR) and 8(SR) and 8(RS), would do exactly the same job producing preferentially the opposite enantiomers, and neither amplifying nor dissipating effects are expected. This mechanism would correlate with the experimental results from entries 9 and 23 (Table 1).



Scheme 9. Computational results (ΔG_{298} and ΔH relative to **7(S) + Zn(i-Pr)₂ + 3**) for the reaction of diisopropyl zinc with aldehyde **3** catalyzed by **8(SS)**. Optical activity is not affected.

The smaller size of the 5-membered heterocycle compared to the pyrimidine or pyridine rings in the classic Soai substrates does not allow for creating a 12-membered macrocycle as the core of the tetrameric cluster. Instead, a 10-membered ring is formed by one coordination N–Zn bond and one hydrogen O–H bond (Scheme 10).

As a result, only one Zn atom in the core remains capable of coordinating $\text{Zn}(i\text{-Pr})_2$, yielding **12(SSSS)**. Either of the two *i*-Pr groups of $\text{Zn}(i\text{-Pr})_2$ can participate in the alkylation (Figure 4). In this case, a preferential formation of the opposite enantiomer **7(R)** from **8(SSSS)** was computed. The π - π stacking due to the practically coplanar orientation of the incoming aldehyde with one of the alcoholate units of the tetramer in **TS3(R)** makes it significantly more stable than **TS3(S)**. Although it is evident that **8(RRRR)** would generate **7(S)** with the same efficiency, a simple analysis shows that in that situation, any existing enantiomeric excess will be degraded to microscopic values. This prediction corresponds to the experimental results from entries 8, 15, 16 and 21 in Table 1.

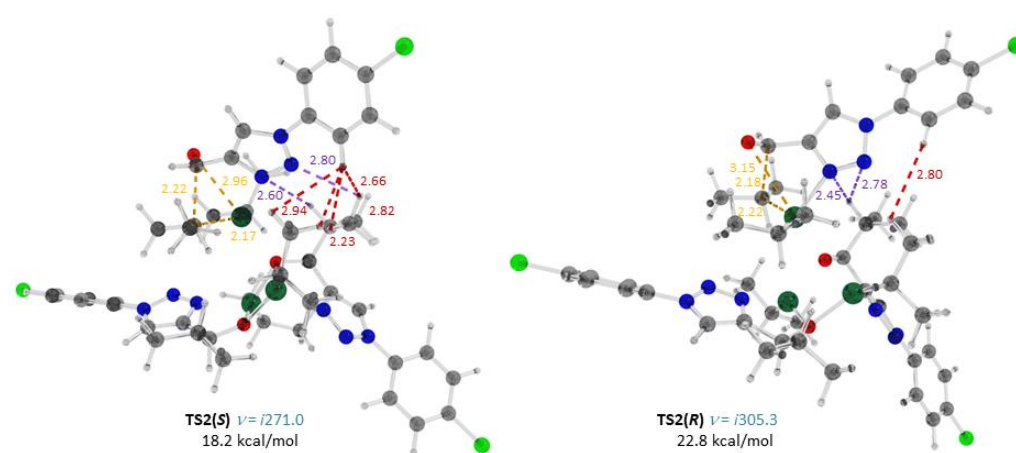
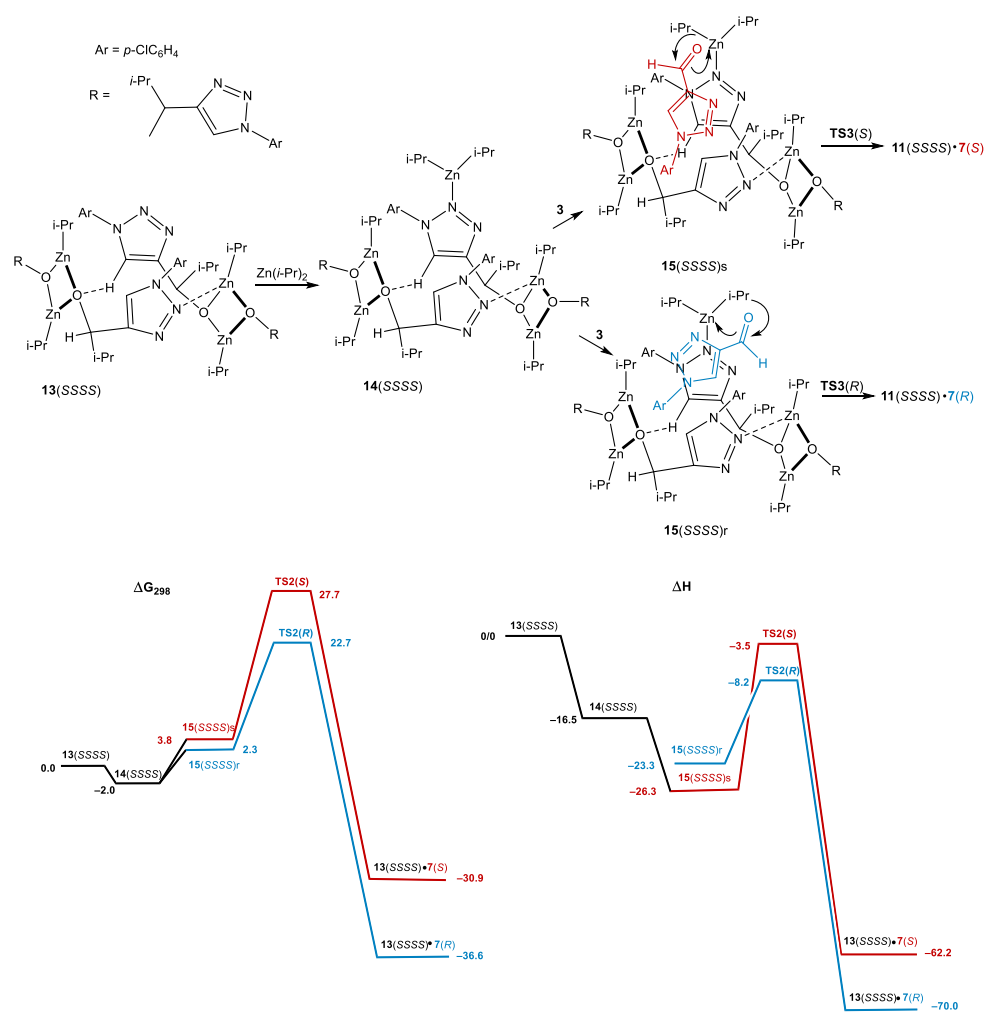


Figure 3. Optimized structures, important interatomic distances (Å) and Gibbs free energies (ΔG_{298} , relative to $2 \mathbf{8}(SS) + \text{Zn}(i\text{-Pr})_2 + \mathbf{3}$) of the transition states **TS2(S)** and **TS2(R)** for the alkylation of **3** catalyzed with **8(SS)**. Atoms: gray—carbon; light gray—hydrogen; red—oxygen; blue—nitrogen; green—chlorine; turquoise—zinc. Interatomic distances: yellow—forming bonds and those being broken; green—Zn—N; blue: CH...O; violet, CH...N; red—CH...HC.



Scheme 10. Computational results (ΔG_{298} , ΔH , kcal/mol relative to **13(SSSS) + Zn(i-Pr)₂ + 3**) for the reaction of diisopropyl zinc with aldehyde **3** catalyzed by **13(SSSS)**. Dissipation of ee.

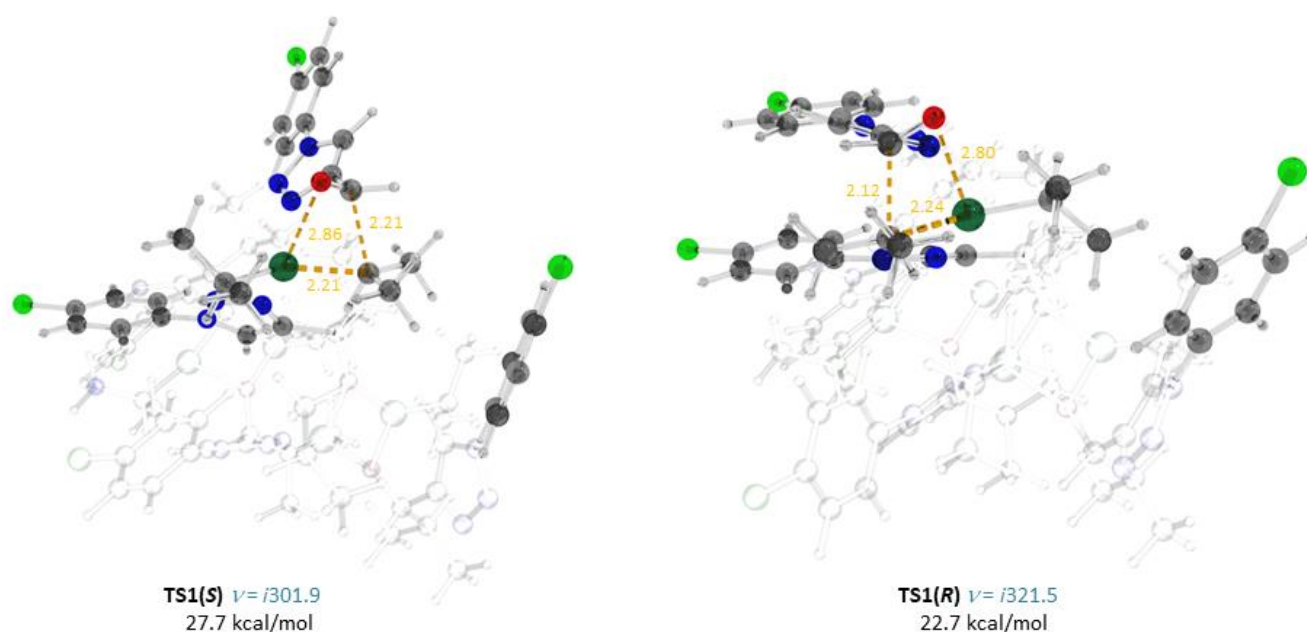


Figure 4. Optimized structures, important interatomic distances (Å) and Gibbs free energies (relative to $13(\text{SSSS}) + \text{Zn}(i\text{-Pr})_2 + 3$) of the transition states TS2(S) and TS2(R) for the alkylation of **3** catalyzed with **8(SS)**. Atoms: gray—carbon; light gray—hydrogen; red—oxygen; blue—nitrogen; green—chlorine; turquoise—zinc. Interatomic distances: yellow—forming bonds and those being broken.

4. Discussion

Our computational results based on the preliminary experimental findings testify to the fact that in the reaction of diisopropyl zinc with triazoles **1–3**, three different regimes of ee changes occur in the course of the reaction: accumulation to detectable amounts, keeping the microscopic ee unchanged and degradation of the macroscopic ee to microscopic values.

This situation must be a much more frequent occurrence compared to the perfect asymmetric auto amplification in the Soai reaction. On the other hand, the evidently increasing randomness of the chiral amplification makes its observation and proper characterization significantly more difficult.

We realize that a much larger set of experimental data would be necessary to claim the achievement of exercising some control over AAA. Extension of the substrates' scope, serial experiments, NMR studies on the reaction pools of these reactions and kinetic simulations based on the computed catalytic cycles are in progress in our laboratories.

Supplementary Materials: The following supporting information can be downloaded at: <https://www.mdpi.com/article/10.3390/sym15071382/s1>. Experimental details, NMR and HPLC charts, computational details, cartesian coordinates for all computed minima and transition states. Table S1: describing changes in the thermodynamic parameters for the intermediates and transition states in the computed catalytic cycles.

Author Contributions: Conceptualization, I.D.G. and A.R.K.; investigation, O.A.M., L.Z.L. and E.S.S.; writing—original draft preparation, I.D.G.; writing—review and editing, A.R.K.; supervision, I.D.G.; project administration, I.D.G.; funding acquisition, I.D.G. All authors have read and agreed to the published version of the manuscript.

Funding: This research was funded by a research grant from Russian Science Foundation #22-13-00275.

Data Availability Statement: Data available on request.

Conflicts of Interest: The authors declare no conflict of interest.

References

1. Soai, K.; Shibata, T.; Morioka, H.; Choji, K. Asymmetric autocatalysis and amplification of enantiomeric excess of a chiral molecule. *Nature* **1995**, *378*, 767–768. [[CrossRef](#)]
2. Mislow, K. Absolute asymmetric synthesis: A commentary. *Collect. Czech. Chem. Commun.* **2003**, *68*, 849–864. [[CrossRef](#)]
3. Soai, K. Asymmetric Autocatalysis, Absolute Asymmetric Synthesis and Origin of Homochirality of Biomolecules. In *Progress in Biological Chirality*; Palyi, G., Zucchi, C., Caglioti, L., Eds.; Elsevier: London, UK, 2004; Volume 1, pp. 355–364.
4. Brown, J.M. Reaction Mechanism in the Study of Amplifying Asymmetric Autocatalysis. In *Asymmetric Autocatalysis: The Soai Reaction*; Soai, K., Kawasaki, T., Matsumoto, A., Eds.; Royal Society of Chemistry: Cambridge, UK, 2022; Volume 43, pp. 97–128.
5. Soai, K.; Sato, I.; Shibata, T.; Komiyama, S.; Hayashi, M.; Matsueda, Y.; Imamura, H.; Hayase, T.; Morioka, H.; Tabira, H.; et al. Asymmetric synthesis of pyrimidyl alkanol without adding chiral substances by the addition of diisopropylzinc to pyrimidine-5-carbaldehyde in conjunction with asymmetric autocatalysis. *Tetrahedron Asymmetry* **2003**, *14*, 185–188. [[CrossRef](#)]
6. Gridnev, I.D.; Serafimov, J.M.; Quiney, H.; Brown, J.M. Reflections on spontaneous asymmetric synthesis by amplifying autocatalysis. *Org. Biomol. Chem.* **2003**, *1*, 3811–3819. [[CrossRef](#)]
7. Singleton, D.A.; Vo, L.K. A Few Molecules Can Control the Enantiomeric Outcome. Evidence Supporting Absolute Asymmetric Synthesis Using the Soai Asymmetric Autocatalysis. *Org. Lett.* **2003**, *23*, 4337–4339. [[CrossRef](#)] [[PubMed](#)]
8. Soai, K.; Shibata, T.; Sato, I. Discovery and Development of Asymmetric Autocatalysis. *Bull. Chem. Soc. Jpn.* **2004**, *77*, 1063–1073. [[CrossRef](#)]
9. Gridnev, I.D.; Vorob'ev, A.K. Quantification of Sophisticated Equilibria in the Reaction Pool and Amplifying Catalytic Cycle of the Soai Reaction. *ACS Catal.* **2012**, *2*, 2137–2149. [[CrossRef](#)]
10. Athavale, S.V.; Simon, A.; Houk, K.N.; Denmark, S.E. Structural Contributions to Autocatalysis and Asymmetric Amplification in the Soai Reaction. *J. Am. Chem. Soc.* **2020**, *142*, 18387–18406. [[CrossRef](#)]
11. Girard, C.; Kagan, H.B. Nonlinear Effects in Asymmetric Synthesis and Stereoselective Reactions: Ten Years of Investigation. *Angew. Chem. Int. Ed.* **1998**, *37*, 2922–2959. [[CrossRef](#)]
12. Song, H.; Rogers, N.J.; Brabec, V.; Clarkson, G.J.; Coverdale, J.P.C.; Kosthunova, H.; Phillips, R.M.; Postings, M.; Shepherd, S.L.; Scott, P. Triazole-based, optically-pure metallocsupramolecules; highly potent and selective anticancer compounds. *Chem. Commun.* **2020**, *56*, 6392–6395. [[CrossRef](#)]
13. Dai, Z.C.; Chen, Y.F.; Zhang, M.; Li, S.K.; Yang, T.-T.; Shen, L.; Wang, J.X.; Qian, S.S.; Zhu, H.L.; Ye, Y.H. Synthesis and antifungal activity of 1,2,3-triazole phenylhydrazone derivatives. *Org. Biomol. Chem.* **2015**, *13*, 477–486. [[CrossRef](#)] [[PubMed](#)]
14. Chai, J.-D.; Head-Gordon, M. Long-Range Corrected Hybrid Density Functionals with Damped Atom–Atom Dispersion Corrections. *Phys. Chem. Chem. Phys.* **2008**, *10*, 6615–6620. [[CrossRef](#)] [[PubMed](#)]
15. Frisch, M.J.; Trucks, G.W.; Schlegel, H.B.; Scuseria, G.E.; Robb, M.A.; Cheeseman, J.R.; Scalmani, G.; Barone, V.; Mennucci, B.; Petersson, G.A.; et al. *Gaussian 09, Rev. D.01*; Gaussian, Inc.: Wallingford, CT, USA, 2013.
16. Becke, A.D. Density-functional exchange-energy approximation with correct asymptotic behavior. *Phys. Rev. A* **1988**, *38*, 3098–3100. [[CrossRef](#)] [[PubMed](#)]
17. Ditchfield, R.; Hehre, W.J.; Pople, J.A. Self-Consistent Molecular-Orbital Methods. IX. An Extended Gaussian-Type Basis for Molecular-Orbital Studies of Organic Molecules. *J. Chem. Phys.* **1971**, *54*, 724–728. [[CrossRef](#)]
18. Hehre, W.J.; Ditchfield, R.; Pople, J.A. Self-Consistent Molecular Orbital Methods. XII. Further Extensions of Gaussian-Type Basis Sets for Use in Molecular Orbital Studies of Organic Molecules. *J. Chem. Phys.* **1972**, *56*, 2257–2261. [[CrossRef](#)]
19. Hariharan, P.C.; Pople, J.A. The influence of polarization functions on molecular orbital hydrogenation energies. *Theor. Chim. Acta* **1973**, *28*, 213–222. [[CrossRef](#)]
20. Francl, M.M.; Pietro, W.J.; Hehre, W.J.; Binkley, J.S.; Gordon, M.S.; DeFrees, D.J.; Pople, J.A. Self-consistent molecular orbital methods. XXIII. A polarization-type basis set for second-row elements. *J. Chem. Phys.* **1982**, *77*, 3654–3665.
21. Gordon, M.S.; Binkley, J.S.; Pople, J.A.; Pietro, W.J.; Hehre, W.J. Self-consistent molecular-orbital methods. Small split-valence basis sets for second-row elements. *J. Am. Chem. Soc.* **1982**, *104*, 2797–2803. [[CrossRef](#)]
22. Rassolov, V.A.; Pople, J.A.; Ratner, M.A.; Windus, T.L. 6-31G * basis set for atoms K through Zn. *J. Chem. Phys.* **1998**, *109*, 1223–1229. [[CrossRef](#)]
23. Marenich, A.V.; Cramer, C.J.; Truhlar, D.G. Universal Solvation Model Based on Solute Electron Density and on Continuum Model of the Solvent Defined by the Bulk Dielectric Constant and Atomic Surface Tensions. *J. Phys. Chem. B* **2009**, *113*, 6378–6396. [[CrossRef](#)]
24. Dheer, D.; Singh, V.; Shankar, R. Medicinal attributes of 1,2,3-triazoles: Current developments. *Bioorg. Chem.* **2017**, *71*, 30–54. [[CrossRef](#)]
25. Schulze, B.; Schubert, U.S. Beyond click chemistry—Supramolecular interactions of 1,2,3-triazoles. *Chem. Soc. Rev.* **2014**, *43*, 2522–2571. [[CrossRef](#)]
26. Liang, L.; Astruc, D. The copper (I)-catalyzed alkyne-azide cycloaddition (CuAAC) “click” reaction and its applications. An overview. *Coord. Chem. Rev.* **2011**, *255*, 2933–2945. [[CrossRef](#)]
27. Ngo, J.T.; Adams, S.R.; Deerinck, T.J.; Boassa, D.; Rodriguez-Rivera, F.; Palida, S.F.; Bertozzi, C.R.; Ellisman, M.H.; Tsien, R.Y. Click-EM for imaging metabolically tagged nonprotein biomolecules. *Nat. Chem. Biol.* **2016**, *12*, 459–465. [[CrossRef](#)]
28. Astruc, D.; Liang, L.; Rapakousiou, A.; Ruiz, J. Click dendrimers and triazole-related aspects: Catalysts, mechanism, synthesis, and functions. A bridge between dendritic architectures and nanomaterials. *Acc. Chem. Res.* **2012**, *45*, 630–640. [[CrossRef](#)]

29. Wang, X.; Huang, B.; Liu, X.; Zhan, P. Discovery of bioactive molecules from CuAAC click-chemistry-based combinatorial libraries. *Drug Discov. Today* **2016**, *21*, 118–132. [[CrossRef](#)] [[PubMed](#)]
30. Bozorov, K.; Zhao, J.; Aisa, H.A. 1,2,3-Triazole-containing hybrids as leads in medicinal chemistry: A recent overview. *Bioorg. Med. Chem.* **2019**, *27*, 3511–3531. [[CrossRef](#)]
31. Zhang, S.; Xu, Z.; Gao, C.; Ren, Q.C.; Chang, L.; Lv, Z.S.; Feng, L.S. Triazole derivatives and their anti-tubercular activity. *Eur. J. Med. Chem.* **2017**, *138*, 501–513. [[CrossRef](#)]
32. Bangalore, P.K.; Vagolu, S.K.; Bollikanda, R.K.; Veeragoni, D.K.; Choudante, P.C.; Misra, S.; Sriram, D.; Sridhar, B.; Kantevari, S. Usnic Acid Enaminone-Coupled 1,2,3-Triazoles as antibacterial and antitubercular Agents. *J. Nat. Prod.* **2019**, *83*, 26–35. [[CrossRef](#)]
33. Manohar, S.; Khan, S.I.; Rawat, D.S. Synthesis of 4-aminoquinoline-1,2,3-triazole and 4-aminoquinoline-1,2,3-triazole-1,3,5-triazine hybrids as potential antimalarial agents. *Chem. Biol. Drug Des.* **2011**, *78*, 124–136. [[CrossRef](#)] [[PubMed](#)]
34. Pribut, N.; Veale, C.G.L.; Basson, A.E.; van Otterlo, W.A.L.; Pelly, S.C. Application of the Huisgen cycloaddition and ‘click’ reaction toward various 1, 2, 3-triazoles as HIV non-nucleoside reverse transcriptase inhibitors. *Bioorg. Med. Chem. Lett.* **2016**, *26*, 3700–3704. [[CrossRef](#)] [[PubMed](#)]
35. Narsimha, S.; Nukala, S.K.; Jyostna, T.S.; Ravinder, M.; Rao, M.S.; Reddy, N.V. One-pot synthesis and biological evaluation of novel 4-[3-fluoro-4-(morpholin-4-yl)] phenyl-1H-1,2,3-triazole derivatives as potent antibacterial and anticancer agents. *J. Heterocycl. Chem.* **2020**, *57*, 1655–1665. [[CrossRef](#)]
36. Buckle, D.R.; Outred, D.J.; Rockell, C.J.M.; Smith, H.; Spicer, B.A. Studies on v-triazoles. 7. Antiallergic 9-oxo-1H,9H benzopyrano[2,3-d]-v-triazoles. *J. Med. Chem.* **1983**, *26*, 251–254. [[CrossRef](#)] [[PubMed](#)]
37. Kant, R.; Kumar, D.; Agarwal, D.; Gupta, R.D.; Tilak, R.; Awasthi, S.K.; Agarwal, A. Synthesis of newer 1,2,3-triazole linked chalcone and flavone hybrid compounds and evaluation of their antimicrobial and cytotoxic activities. *Eur. J. Med. Chem.* **2016**, *113*, 34–49. [[CrossRef](#)] [[PubMed](#)]
38. Gridnev, I.D.; Serafimov, J.M.; Brown, J.M. Solution Structure and Reagent Binding of the Zinc Alkoxide Catalyst in the Soai Asymmetric Autocatalytic Reaction. *Angew. Chem. Int. Ed.* **2004**, *43*, 4884–4887. [[CrossRef](#)]

Disclaimer/Publisher’s Note: The statements, opinions and data contained in all publications are solely those of the individual author(s) and contributor(s) and not of MDPI and/or the editor(s). MDPI and/or the editor(s) disclaim responsibility for any injury to people or property resulting from any ideas, methods, instructions or products referred to in the content.